JOURNAL OF ENVIRONMENTAL SCIENCES XX (2018) XXX–XXX

Available online at www.sciencedirect.com

ScienceDirect

www.elsevier.com/locate/jes

JES JOURNAL OF ENVIRONMENTAL SCIENCES

www.jesc.ac.cn

Investigating missing sources of glyoxal over China using a regional air quality model (RAMS-CMAQ)

Jialin Li[1,2], *Meigen Zhang*[1,2,3,*], *Guiqian Tang*[1], *Fangkun Wu*[1], *Leonardo M.A. Alvarado*[4], *Mihalis Vrekoussis*[4,5,6], *Andreas Richter*[4], *John P. Burrows*[4]

1. *State Key Laboratory of Atmospheric Boundary Layer Physics and Atmospheric Chemistry (LAPC), Institute of Atmospheric Physics (IAP), Chinese Academy of Sciences (CAS), Beijing 100029, China*
2. *University of Chinese Academy of Sciences, Beijing 100049, China*
3. *Center for Excellence in Urban Atmospheric Environment, Institute of Urban Environment, Chinese Academy of Sciences, Xiamen 361021, China*
4. *Institute of Environmental Physics and Remote Sensing, IUP, University of Bremen, D-28203 Bremen, Germany*
5. *Center of Marine Environmental Sciences, MARUM, University of Bremen, D-28203 Bremen, Germany*
6. *Energy, Environment and Water Research Center, the Cyprus Institute, CY2121 Nicosia, Cyprus*

ARTICLE INFO

Article history:
Received 31 July 2017
Revised 17 April 2018
Accepted 19 April 2018
Available online xxxx

Keywords:
Glyoxal
Volatile organic compounds
Molar yields
RAMS-CMAQ
China

ABSTRACT

Currently, modeling studies tend to significantly underestimate observed space-based glyoxal (CHOCHO) vertical column densities (VCDs), implying the existence of missing sources of glyoxal. Several recent studies suggest that the emissions of aromatic compounds and molar yields of glyoxal in the chemical mechanisms may both be underestimated, which can affect the simulated glyoxal concentrations. In this study, the influences of these two factors on glyoxal amounts over China were investigated using the RAMS-CMAQ modeling system for January and July 2014. Four sensitivity simulations were performed, and the results were compared to satellite observations. These results demonstrated significant impacts on glyoxal concentrations from these two factors. In case 1, where the emissions of aromatic compounds were increased three-fold, improvements to glyoxal VCDs were seen in high anthropogenic emissions regions. In case 2, where molar yields of glyoxal from isoprene were increased five-fold, the resulted concentrations in July were 3–5-fold higher, achieving closer agreement between the modeled and measured glyoxal VCDs. The combined changes from both cases 1 and 2 were applied in case 3, and the model succeeded in further reducing the underestimations of glyoxal VCDs. However, the results over most of the regions with pronounced anthropogenic emissions were still underestimated. So the molar yields of glyoxal from anthropogenic precursors were considered in case 4. With these additional mole yield changes (a two-fold increase), the improved concentrations agreed better with the measurements in regions of the lower reaches of the Yangtze River and Yellow River in January but not in July.

* *Corresponding author. E-mail address:* mgzhang@mail.iap.ac.cn (Meigen Zhang).

https://doi.org/10.1016/j.jes.2018.04.021
1001-0742/

Introduction

Organic aerosol (OA) accounts for a large fraction of fine particulate matter (20%–90%) (Kanakidou et al., 2005), and has significant impacts on atmospheric chemistry, air quality, and climate (Fu et al., 2008). OA can be classified into primary organic aerosol (POA) and secondary organic aerosol (SOA). The former is directly emitted through the combustion of anthropogenic and biogenic sources, while the latter is produced through the oxidation of volatile organic compounds (VOCs), followed by the partition of semi-volatile organic compounds (SVOCs) into the aerosol phase (Fuzzi et al., 2006; Seinfeld and Pankow, 2003). However, studies have shown that SOA is underpredicted in models by a factor between 8 and 100 (de Gouw et al., 2005; Volkamer et al., 2006), resulting in underestimation of OA (Fu et al., 2012; Jiang et al., 2012; Li et al., 2017a; Lin et al., 2016; Matsui et al., 2014; Utembe et al., 2011). One of the reasons for this is the uncertainty in emission sources of VOC precursors (Carlton et al., 2009; Goldstein and Galbally, 2007; Li et al., 2017a).

Glyoxal, one of the most prevalent dicarbonyl compounds in the atmosphere, has been identified as a potentially important precursor of SOA through aqueous-phase chemical processes (Altieri et al., 2008; Carlton et al., 2007, 2006; Lim and Ziemann, 2005; Zhao et al., 2006). Although glyoxal can be directly emitted during biofuel combustion and biomass burning (Fu et al., 2008), it is primarily produced through the oxidation of hydrocarbons with no fewer than two carbon atoms (Calvert et al., 2000, 2002). Due to the lack of information about the distribution of direct and indirect sources of glyoxal (Vrekoussis et al., 2009), large uncertainties exist regarding the sources of glyoxal. Recent studies have reported a substantially underestimated glyoxal vertical column density (VCD) (Fu et al., 2008; Myriokefalitakis et al., 2008; Liu et al., 2012), and this discrepancy, which may potentially contribute to the underestimation of SOA, implies the existence of additional sources, or an underestimation in the known sources of glyoxal (Stavrakou et al., 2009). However, few studies have investigated this further. Stavrakou et al. (2009) investigated this discrepancy using an inversion scheme to constrain the missing indirect and direct sources of glyoxal based on glyoxal and formaldehyde columns observed by the SCIAMACHY sensor. However, this approach introduced a number of new uncertainties such as unspecified glyoxal precursors, assumptions in the emissions rate, *etc.* A few years later, Liu et al. (2012) used space-based SCIAMACHY (SCanning Imaging Absorption spectroMeter for Atmospheric CHartographY) glyoxal VCDs and the Regional Chemical Transport Model to show that the discrepancy between the simulated and the observed glyoxal amounts emanates from a substantial underestimation in the aromatic emission inventories. They concluded that "the specific causes for the large underestimation of aromatics emissions merit further investigations".

In the present study, four sensitivity simulations were performed with the RAMS-CMAQ (the Regional Atmospheric Modeling system coupled with Community Multiscale Air Quality modeling system) modeling system to examine the potential impacts on glyoxal VCDs over China of two factors, namely, the molar yields of glyoxal in the chemical mechanisms (F_{YIE}, discussed here for the first time), and the emissions of aromatic compounds (F_{EMIS}). The base model settings and the observation data are described in Section 1. In Section 2, the model performances are evaluated, and the influences of the two factors on glyoxal VCDs are discussed through comparisons between the results of the simulation cases and satellite measurements. The study's conclusions are summarized in Section 3.

1. Model and data

1.1. *Base model settings*

CMAQ version 4.7.1 was chosen as the base model, configured with the gas chemical mechanism, SAPRC99 (1999 Statewide Air Pollutant Research Center) (Carter, 2000), to assess the contributions of the two missing sources of glyoxal. In this version, glyoxal production from hydrocarbons was accounted for, where the precursors included isoprene, terpene, propane and acetylene (combined as ALK2), ethylene, toluene (combined with other aromatics as ARO1), xylene (combined with other aromatics as ARO2), and phenol. Along sinks due to photolysis and oxidation by OH/NO_3 radicals, another important glyoxal sink is its role in the formation of in-cloud SOA, which was also incorporated into the model (Carlton et al., 2008). The aqueous chemistry, subgrid clouds, and scavenging processes (both within and below clouds) were parameterized in the cloud module, in a similar way as in RADM (Regional Acid Deposition Model) (Chang et al., 1987).

The meteorological fields from RAMS were read into CMAQ to drive the model. A detailed description of RAMS and its capabilities is given by Cotton et al. (2003). In this study, RAMS has been operated in the four-dimensional data assimilation mode using nudging analysis. The synoptic meteorological fields used in RAMS were the National Centers for Environmental Predictions (NCEP) datasets (temporal resolution: 6 hr; spatial resolution: 1° × 1°). Weekly mean sea surface temperature (SST) and monthly observed snow cover information were used as the boundary conditions for the RAMS computations.

Anthropogenic emissions, including power, industry, residential, transportation and agriculture, were adopted from the monthly emissions inventory for the base year of 2012 with a spatial resolution of 0.25° × 0.25°, and chemical species included in the inventory were black carbon (BC), organic carbon (OC), SO_2, NO_x, CO, non-methane VOCs (NMVOCs), NH_3 and other particulate matters (Li et al., 2017b). Speciation of NMVOCs compatible with SAPRC99 was also provided (Li et al., 2014). More details can be found at http://www.meicmodel.org. Biogenic emissions were derived from the Model of Emissions of Gases and Aerosols from Nature (MEGAN) (Guenther et al., 2012). The Global Emissions Inventory Activity (GEIA) (a 1° × 1° monthly inventory) (Benkovitz et al., 1996) provided the lighting NO_x, while the open biomass burning emissions were obtained from the Global Fire Emissions Database, Version 4 (Randerson et al., 2015). Dust emissions were calculated online with an empirical dust model developed by Han et al. (2004) and sea salt by the scheme of Gong (2003), respectively. The Model of Ozone and Related Tracers, version 4 (MOZART-4) (Emmons et al., 2010) provided the boundary conditions for the model calculation.

Please cite this article as: Li, J., et al., Investigating missing sources of glyoxal over China using a regional air quality model (RAMS-CMAQ), J. Environ. Sci. (2018), https://doi.org/10.1016/j.jes.2018.04.021

The model domain was 6656 × 5440 km^2 on a rotated polar-stereographic map projection centered at (35°N, 110°E) (shown in Fig. 1). The horizontal resolution was 64 km. The blue box in Fig. 1 shows the region of interest. The vertical dimension of the CMAQ simulation was divided into 15 layers and extended from the surface to approximately 23 km high, with the lowest 7 layers in the bottom 2 km to resolve the planetary boundary layer.

1.2. Observational data

The observational data used in this study were derived from satellite and surface measurements taken in 2014. To evaluate the emission biases of aromatic compounds, comparisons were made between simulated and observed concentrations, according to Zhang and Ying (2011). Aromatic compound concentrations were measured every Thursday at 14:00 local standard time (LST) with a gas chromatography mass spectrometer (GC–MS) at three sites (Beijing, Xinglong, and Yucheng; shown in Fig. 1). The detailed methods of sampling and analysis are given in Sun et al. (2016) and Wu et al. (2016).

To determine the impacts of the molar yields of glyoxal in the chemical mechanisms and the emissions of aromatic compounds on glyoxal, the mean tropospheric glyoxal vertical column abundances for each month were calculated from satellite measurements using the Ozone Monitoring Instrument (OMI) (Levelt et al., 2006). A detailed description of the glyoxal retrieval technique, the updated differential optical absorption spectroscopy (DOAS) method, is given by Alvarado et al. (2014), which accounts for different interferences species in the wavelength range and is one part of a homogenized retrieval from multiple satellite platforms as described in Alvarado (2016). To constrain the sources of glyoxal, space-based formaldehyde (HCHO) measurements were utilized, since the two gases have common precursors (isoprene, terpene, ethylene, and ALK2 in our model) and are correlated through chemistry. The data of monthly mean tropospheric HCHO VCDs retrieved from the OMI instrument were obtained from the Tropospheric Emissions Monitoring Internet Service (TEMIS) and the relevant data information can be found in De Smedt et al. (2015). Due to the difficulty in retrieving glyoxal columns over oceans [caused by interference from liquid water absorption (Alvarado et al., 2014; Lerot et al., 2010; Wittrock et al., 2006)], and to the fact that the HCHO columns over oceanic areas lie close to the detection limit of the instrument, the main focus of this study was limited to continental regions. In order to evaluate the impacts of NO_2 concentrations on the ratios between averaged glyoxal and formaldehyde VCDs (R_{GF}) (the detailed impacts of NO_2 on R_{GF} are described in Section 2.2), tropospheric NO_2 columns derived from the OMI instrument were obtained from the NASA Goddard Earth Sciences (GES) Data and Information Services Center (DISC) (http://disc.sci.gsfc.nasa.gov/data/Aura_OMI _Level3/OMNO2d.003/2014) and the detailed product information are given in Krotkov et al. (2016).

To evaluate the performance of RAMS-CMAQ, the simulated meteorological factors, including temperature (*T*), relative humidity (RH), wind speed (WS), wind direction (WD), and $PM_{2.5}$ concentrations were compared to the measurements over 10 stations (presented in Fig. 1). The hourly observations of meteorological parameters were collected from the Meteorological Information Comprehensive Analysis and Process System (MICAPS), while the hourly observed $PM_{2.5}$ data were derived from the Chinese National Environmental Monitoring Center (CNEMC).

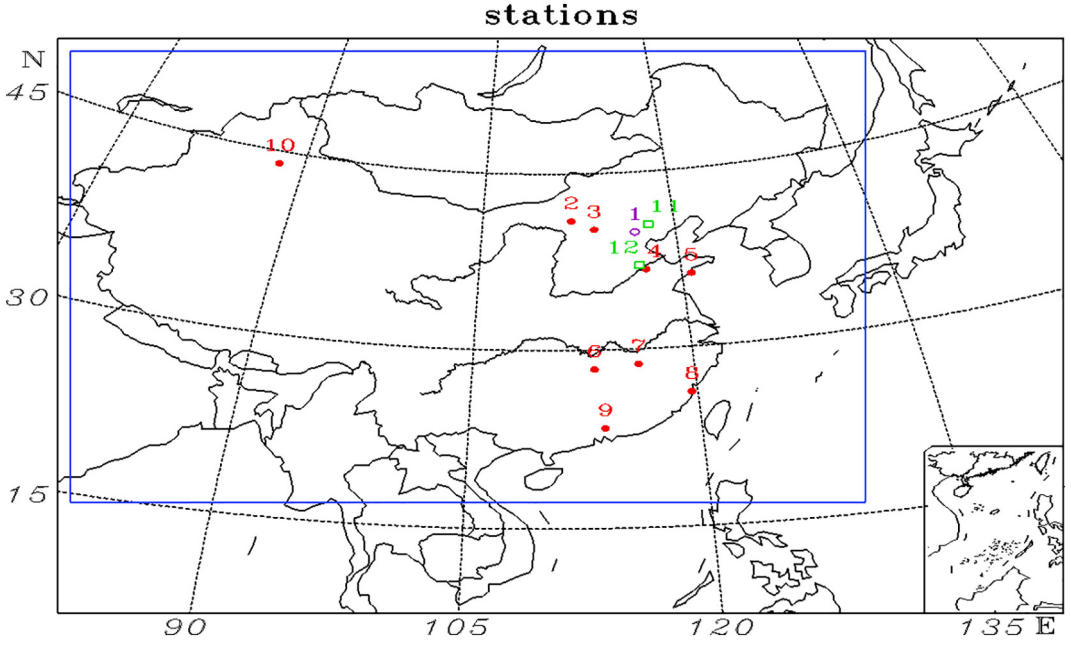

Fig. 1 – Geographic locations of the measurement stations in the model domain. 1: Beijing; 2: Hohhot; 3: Datong; 4: Jinan; 5: Qingdao; 6: Changsha; 7: Nanchang; 8: Fuzhou; 9: Guangzhou; 10: Urumqi; 11: Xinglong; 12: Yucheng. The colored shapes denote which parameters were compared at each station: red filled circle: meteorological parameters; green blank rectangle: aromatic compound concentrations; purple blank circle: both meteorological parameters and aromatic compound concentrations.

Please cite this article as: Li, J., et al., Investigating missing sources of glyoxal over China using a regional air quality model (RAMS-CMAQ), J. Environ. Sci. (2018), https://doi.org/10.1016/j.jes.2018.04.021

2. Results and discussion

Due to the spatial and temporal variability in the emissions of aromatic compounds, the impacts of corresponding emissions biases need to be considered for different seasons. The summer and winter cases were selected because the dominant sources in these two seasons are from biogenic and anthropogenic emissions, respectively. January and July were selected for investigation. The simulations periods were from 0000 UTC 29 December 2013 to 2300 UTC 31 January 2014, and from 0000 UTC 27 June to 2300 UTC 31 July 2014, with the first three days of each period being the spin-up time.

2.1. Model evaluation

Table 1 presents statistical summaries of the meteorological parameters and the $PM_{2.5}$ concentrations in January and July 2014.

For meteorological parameters, due to the limited resolution of the model, several under- and overestimates still existed in the simulated results. However, in the aggregate, the model successfully reproduced the temporal variations in the surface temperature, RH, and wind speed (shown in Figs. S1–S3), with the IOAs of these parameters reaching 0.96, 0.83 and 0.63 in January, and 0.91, 0.87 and 0.61 in July, respectively. These were comparable to the results obtained by Feng et al. (2016). The MBs of the three parameters were 0.09°C, 0.61% and −0.07 m/sec in January, and −0.53°C, 0.53% and −0.46 m/sec in July, respectively, indicating small biases. The RMSEs of *T* and RH were 3.38°C and 16.45% in January, and 2.50°C and 15.19% in July, respectively, comparable to the results of Gao et al. (2016), indicating a reasonable performance of the model. The RMSEs of wind speed fulfilled the performance criteria ($|RMSE| \leq 2$ m/sec) proposed by Emery et al. (2001). Although wind directions (Fig. S4) were not reproduced that well compared to the other three factors, $P_{22.5}°$ and $P_{45}°$ were 26.91% and 46.71% in January, and 29.17% and 50.00% in July, respectively, also implying a reasonable performance by the model for WD. Overall, the model performed well in simulating the meteorological parameters, which ensured reliability for the following simulations.

Table 1 – Performance statistics for meteorological parameters and $PM_{2.5}$.

Variable	Month	N	C_{mod}	C_{obs}	MB	RMSE	IOA
T (°C)	Jan.	4072	1.20	1.11	0.09	3.38	0.96
	Jul.	5386	25.79	26.32	−0.53	2.5	0.91
RH (%)	Jan.	4072	55.98	55.37	0.61	16.45	0.83
	Jul.	5386	68.49	67.96	0.53	15.19	0.87
WS (m/sec)	Jan.	4072	2.16	2.23	−0.07	1.84	0.63
	Jul.	5386	1.75	2.21	−0.46	1.75	0.61
Variable	Month	N	C_{mod}	C_{obs}	FB (%)	FE (%)	IOA
$PM_{2.5}$ (μg/m^3)	Jan.	6513	112.91	100.53	7.99	56.13	0.76
	Jul.	5902	62.54	46.27	15.83	64.04	0.64
Variables	Month		N	$P_{22.5}°$ (%)		$P_{45}°$ (%)	
WD (°)	Jan.		4072	26.91		46.71	
	Jul.		5386	29.17		50.00	

N: total sample quantity; C_{mod} and C_{obs}, mean modeled and observed values, respectively; IOA, index of agreement; MB, mean bias; FB, fractional bias; RMSE, root-mean-square error; FE, fractional error; $P_{22.5}°$ and $P_{45}°$, percentages of the comparison points at which the absolute biases between the modeled and observed WD are within 22.5° and 45°, respectively. The definitions of these statistical parameters are given by Juda-Rezler et al. (2012).

The corresponding comparisons for $PM_{2.5}$ are presented in Fig. S5. The model overestimated $PM_{2.5}$ compared to the observations, probably due to the uncertainties in the emissions inventory, impacts of background transport, and the inherent limitation of the model resolution. However, the system performed well in capturing the variations in $PM_{2.5}$, especially in January, when pollution was more pronounced and appeared more frequently. As presented in Table 1, the IOA of $PM_{2.5}$ reached 0.76 and 0.64 in January and July, respectively, indicating good agreement of the fine particle matter simulations with measurements. Moreover, both the FBs and FEs of $PM_{2.5}$ in January and July were within the performance criteria ($|FB| \leq 60\%$, $FE \leq 75\%$) proposed by Boylan and Russell (2006). This indicated that the model performed reasonable simulations of chemical species, both spatially and temporally.

Table 2 – Sensitivity studies performed to verify the impacts of two underestimated factors.

Sensitivity simulation	Description
Case 1	To examine the impacts of aromatics emissions: increase the emissions of ARO1 in July and ARO2 in January and July by a factor of 3
Case 2	To examine the impacts of molar yields of glyoxal from biogenic precursors: increase the relevant molar yields by a factor of 5
Case 3	To examine both the impacts in cases 1 and 2
Case 4	To examine the molar yields of glyoxal from anthropogenic precursors based on case 3: increase the relevant more yields by a factor of 2

2.2. Sensitivity simulations and analyses

Before examining the influence of F_{YIE} and F_{EMIS} studied in this work, the original simulations (base case) in the model were investigated and compared to observations. Fig. 2 shows the observed and simulated monthly mean tropospheric glyoxal and HCHO VCDs for January and July 2014.

As presented in Fig. 2, the model generally underestimated the glyoxal vertical column densities over the selected region. Even so, the simulated glyoxal columns showed similar patterns as those retrieved from the OMI observations. Over China, in January, the highest values (generally (3–5) × 10^{14} molecules/cm^2) were observed in areas including the Sichuan Basin, south of the middle and lower reaches of the Yangtze River, and the North China Plain (NCP), while the modeled values over these regions were (0.5–3) × 10^{14} molecules/cm^2 (underestimated by a factor between 2 and 10). The lowest measured values (generally less than 2 × 10^{14} molecules/cm^2) appeared in the western regions of China, and were again underestimated by the simulations. In July, the highest VCDs were concentrated in the regions of the Sichuan Basin, NCP and the Yangtze River Delta (YRD), and

Please cite this article as: Li, J., et al., Investigating missing sources of glyoxal over China using a regional air quality model (RAMS-CMAQ), J. Environ. Sci. (2018), https://doi.org/10.1016/j.jes.2018.04.021

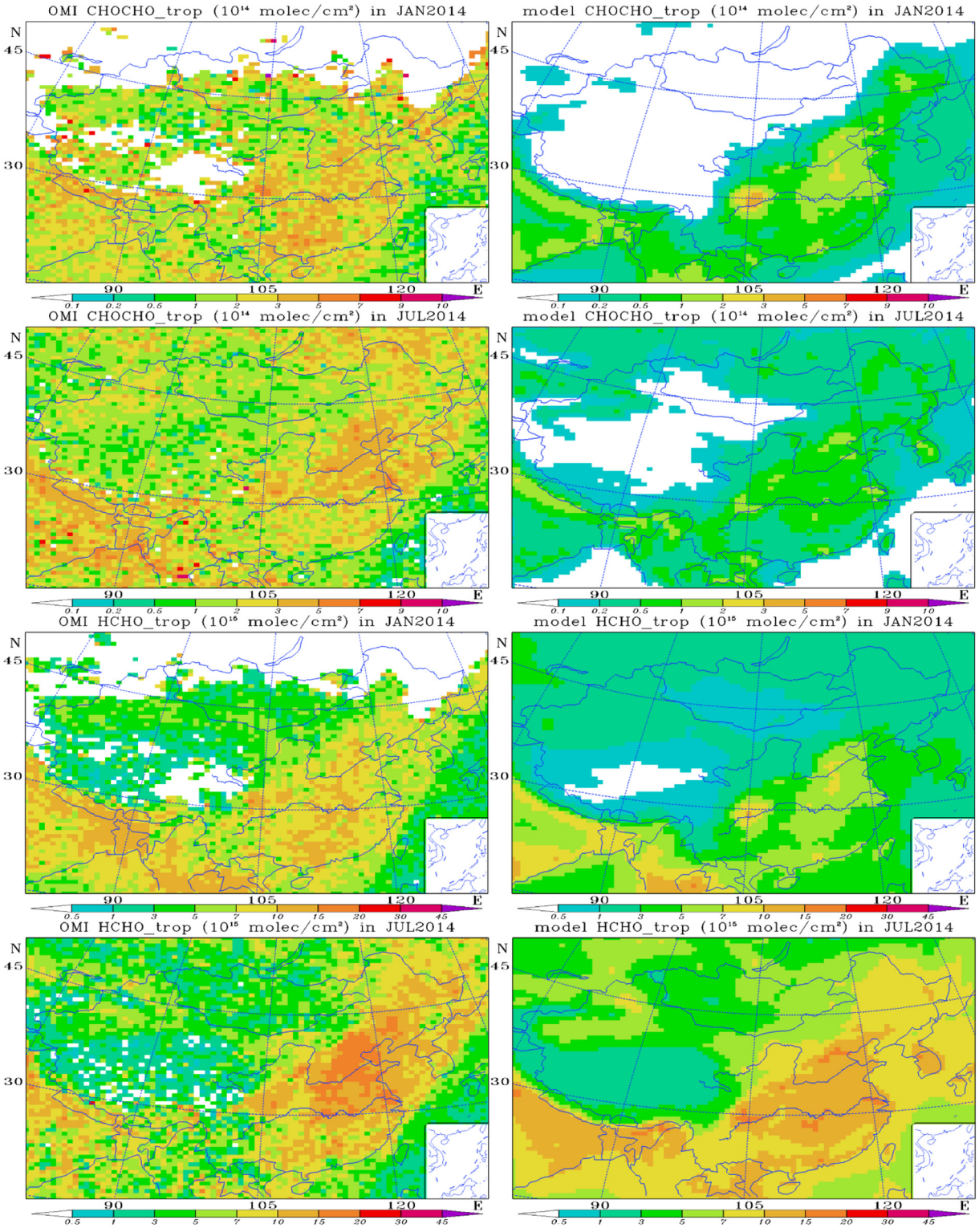

Fig. 2 – Observed and simulated monthly mean tropospheric glyoxal and HCHO VCDs (molecules/cm^2) for January and July 2014 (left: OMI observations; right: base case simulations).

were higher than the modeled results by a factor between 4 and 10. Similarly, in the western regions, the measurements were up to 20 times higher than the simulations. Outside China, high values were seen over northeast India, both in January and July, with a 2–8-fold difference between the observed and simulated quantities. When comparing HCHO, the results over the region showed that the model captured the spatial pattern of the observed HCHO columns in both January and July, and was quite

Please cite this article as: Li, J., et al., Investigating missing sources of glyoxal over China using a regional air quality model (RAMS-CMAQ), J. Environ. Sci. (2018), https://doi.org/10.1016/j.jes.2018.04.021

successful in reproducing the intensity of the measurements in July, except over several high concentration areas (*e.g.*, the NCP, with high population densities).

Following these comparisons, four sensitivity cases (cases 1 to 4) were designed to examine the impacts of two underestimated factors: the emissions of aromatic compounds and the molar yields of glyoxal from precursors. These cases are described in Table 2 and the reasons are explained in the following text.

For case 1, the potential underestimations in the emissions of aromatic compounds for different seasons were first identified and discussed. Fig. 3 shows the ratio of the observed to base case predicted concentrations (O/P ratio) of ARO1 and ARO2 for January and July. As seen in Fig. 3a, in January, with the current emission rates of aromatic compounds, the mean differences in measured and modeled ARO1 were not obvious, while the mean O/P ratios of ARO2 were around 2. In July, the O/P ratios of both ARO1 and ARO2 showed large biases. The mean O/P ratio of ARO1 was comparable to the median value and close to 2, while the mean ratio of ARO2 was as high as 16. This clearly demonstrated underestimations in the emissions of aromatic compounds, both in January and July. Referring to the results of Liu et al. (2012) (who reported emissions underestimated by a factor between 4 and 10), and considering the limited availability of observations and the nonlinear relationship between emissions and final concentrations, the increase in the emission rate of ARO1 was conservatively estimated to be a factor of 3 in July, while the emissions of ARO2 were conservatively estimated to have increased by the same scale both in January and July, for the purposes of the simulation in case 1. The corresponding O/P ratios of case 1 are shown in Fig. 3b. As presented, the mean differences in measured and modeled ARO2 in January were smaller and the mean O/P ratio was around 1. In July, the O/P ratios of both ARO1 and ARO2 were much more concentrated. The mean O/P ratio of ARO1 comparable to the median value was close to 1, while both the mean ratio and the median value of ARO2 significantly decreased. All of these indicated the reasonable increases in the emissions of aromatic compounds in the emission inventory. The final results of glyoxal VCDs in case 1 are shown in Fig. 5a, b. Compared to the original results, glyoxal VCDs for the two months in case 1 were improved. The areas of highest concentrations during the two months were extended from the North China Plain to the south of the Yangtze River, especially in January, and the corresponding concentrations in these areas were increased by a factor of almost 2, contributing to more distinct distributions, which were similar to the observations. However, biases still existed in the results of case 1.

According to Vrekoussis et al. (2010), the ratio between glyoxal and formaldehyde VCDs decreased when the NO_2 column amounts increased. A value of R_{GF} below 0.03 indicated higher HCHO production from anthropogenic precursors, while values between 0.04 and 0.06 implied that the biogenic precursors favored glyoxal production. Since there was good agreement between the observed and base case–simulated NO_2 VCDs over the region (shown in Fig. S6), the R_{GF} in the model was not much affected by NO_2. However, the results of R_{GF} in the base case were quite different from the observations in 2014 (Fig. 4). In January, with the exception of areas where the ratios were more than 0.09, most of the observed ratios were greater than 0.03, and sometimes as large as 0.06. The simulated results, however, showed ratios of less than 0.03 over most of these regions, which indicated that glyoxal derived from biogenic precursors had been underestimated. In July, the simulated ratios over these areas were mostly less than 0.01, while the observations (except for the value of more than 0.09) were mostly greater than 0.03 and as much as 0.06, demonstrating again that the model underestimated the contributions from biogenic sources to glyoxal. The results of R_{GF} in case 1 (presented in Fig. S7a, b) further supported this conclusion though the ratios in several high concentration regions were more than 0.03 in January for the underestimated HCHO VCDs (presented in Fig. S7e). In addition, as shown in Fig. 2, though the HCHO VCDs were underestimated in January, the comparable intensities of HCHO column concentrations between simulations and observations in July, when was dominated by biogenic sources emissions, suggested that the emissions of isoprene and terpene in the inventory were close to the actual emissions over most of the regions during this month. Stavrakou et al. (2009) suggested that underestimations in modeled glyoxal column concentrations might originate from a missing secondary source accounting for

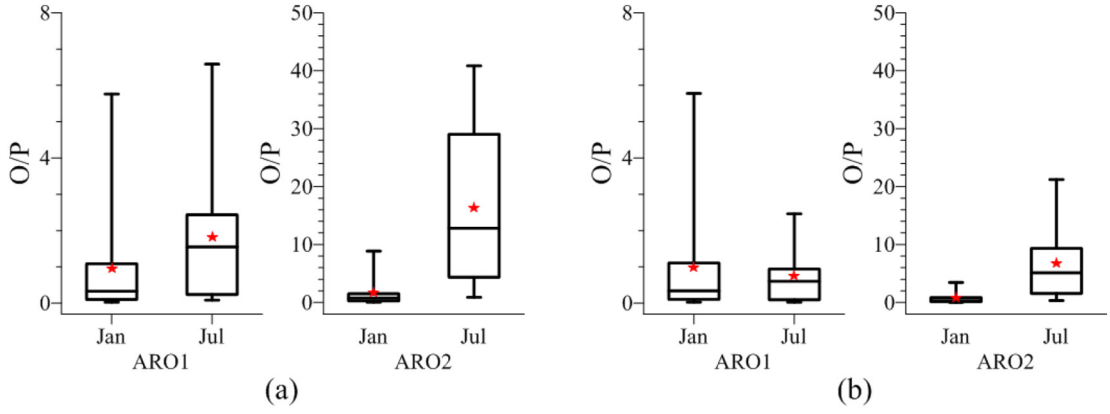

Fig. 3 – Box and whisker plots of the observation to prediction (O/P) ratios for aromatics during January and July 2014. (a) base case; (b) case 1. The observed concentrations were measured every Thursday at 14:00 LST through gas chromatography–mass spectrometry (GC–MS) at three sites (Beijing, Xinglong, and Yucheng). The red stars in the plot represent the average O/P ratios.

Please cite this article as: Li, J., et al., Investigating missing sources of glyoxal over China using a regional air quality model (RAMS-CMAQ), J. Environ. Sci. (2018), https://doi.org/10.1016/j.jes.2018.04.021

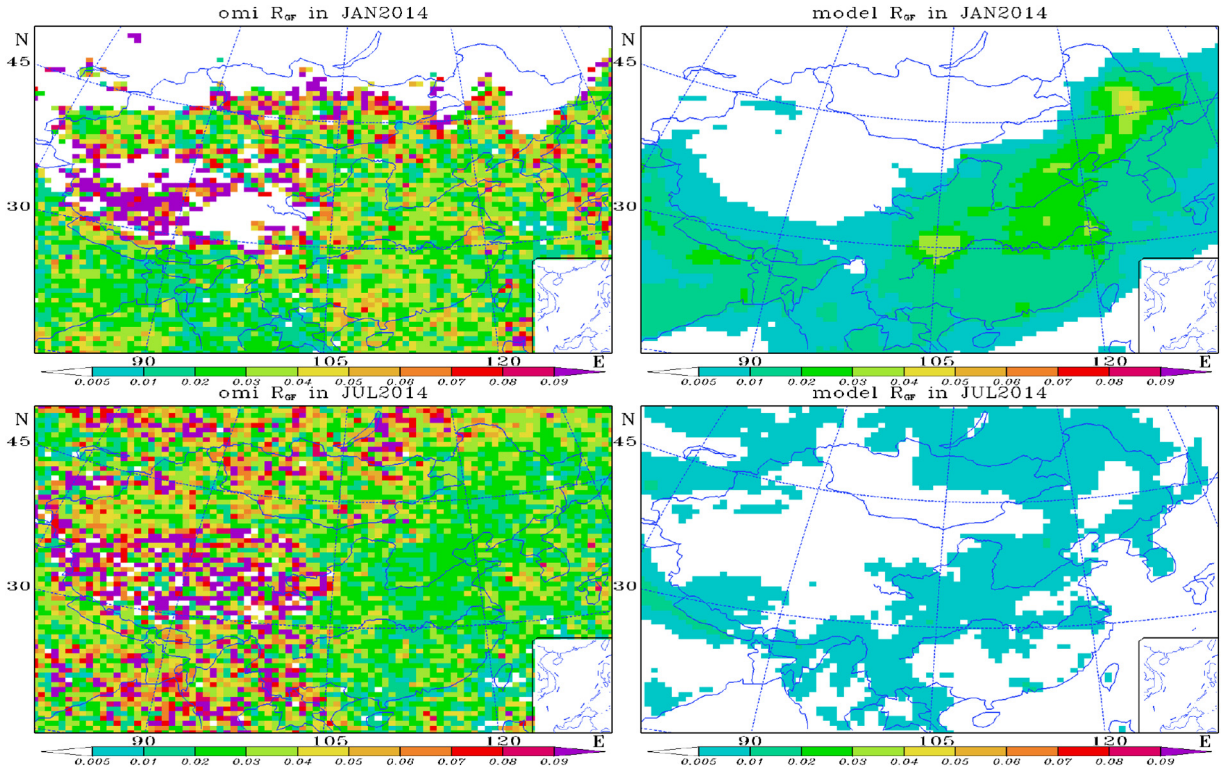

Fig. 4 – Distribution of observed and simulated R_{GF} (ratio between averaged glyoxal and formaldehyde VCDs) in January and July 2014 (left: observations; right: base case simulations).

around 50% of the global budget. It was therefore inferred that the glyoxal molar yields from the biogenic precursors in the chemical mechanism were underestimated.

There were minor contribution to glyoxal from terpene (Liu et al., 2012), and different studies (Archibald et al., 2010; Butler et al., 2008; Kuhn et al., 2007; Lelieveld et al., 2008; Peeters and Muller, 2010; Peeters et al., 2009; Stavrakou et al., 2010; Zhang and Kamens, 2012) indicated the need of substantial revisions in the degradation mechanisms of isoprene oxidations, which may result in the quite different yields of glyoxal from isoprene (Stavrakou et al., 2009). Thus this study only discussed the molar yields of glyoxal from isoprene. In case 2, the molar yields of glyoxal from isoprene, which contributed globally 47% of glyoxal (Fu et al., 2008), were increased by a factor of 5 (a half of the upper limit in the range of 2 to 10) and the corresponding results are presented in Fig. 5c, d. In January, there were no great changes, except for overestimates in areas of Myanmar, Thailand, and eastern India, which may be due to uncertainties in the emissions. In July, the modeled results were quite different from the base simulations, especially the high value ((3–5) × 10^{14} molecules/cm^2) regions (*e.g.*, some parts of eastern India, north of Myanmar, Bhutan, south of Shanxi Province, Sichuan Basin, *etc.*). The distributions in glyoxal VCDs were qualitatively reproduced, with distinct patterns similar to the satellite observations. The different results in January and July were due to the different dominant impact factors in the respective seasons. Due to the low emissions of biogenic precursors in winter over China, the impacts in January were not that obvious. Thus, it can be concluded that the molar yields of glyoxal from isoprene in the chemical mechanism of the model were underestimated and needed to be reconsidered based on the results from July. The R_{GF} in case 2 (shown in Fig. S7c, d) also favored this conclusion.

Based on the results from cases 1 and 2, both impact factors were considered in case 3. As shown in Fig. 5e, f, the changes to glyoxal VCDs in case 3 were similar to those in case 2, but with several key differences, especially in the regions dominated by anthropogenic emissions. In January for case 3, the regions with relatively high values ((2–3) × 10^{14} molecules/cm^2) over the NCP were extended due to the increase in emissions of aromatic compounds, which further reduced the biases compared to observations. Similarly, in July, the areas of high concentrations ((3–5) × 10^{14} molecules/cm^2) were also enlarged. These areas included the Sichuan Basin, several fragmentary regions over the NCP, and the areas around the middle reaches of the Yangtze River, where the anthropogenic source emissions were relatively significant.

Although the results for case 3 were better than those of the other cases, the simulations of glyoxal VCDs in the regions of the lower reaches of the Yangtze River and Yellow River (*e.g.*, the regions of NCP and YRD), where major population centers are located, were not satisfying, especially for the intensities in July (which were underestimated by a factor of 2 to 3). Given that there were high population densities in these areas, two reasons for the remaining discrepancies were considered, namely, the possibility that the emissions of anthropogenic precursors were still underestimated (F1) and the uncertainties in the yields of glyoxal from anthropogenic precursors (F2). The emissions of aromatic compounds were considered first. From the results in Fig. 3b, the emissions of aromatic compounds in

Please cite this article as: Li, J., et al., Investigating missing sources of glyoxal over China using a regional air quality model (RAMS-CMAQ), J. Environ. Sci. (2018), https://doi.org/10.1016/j.jes.2018.04.021

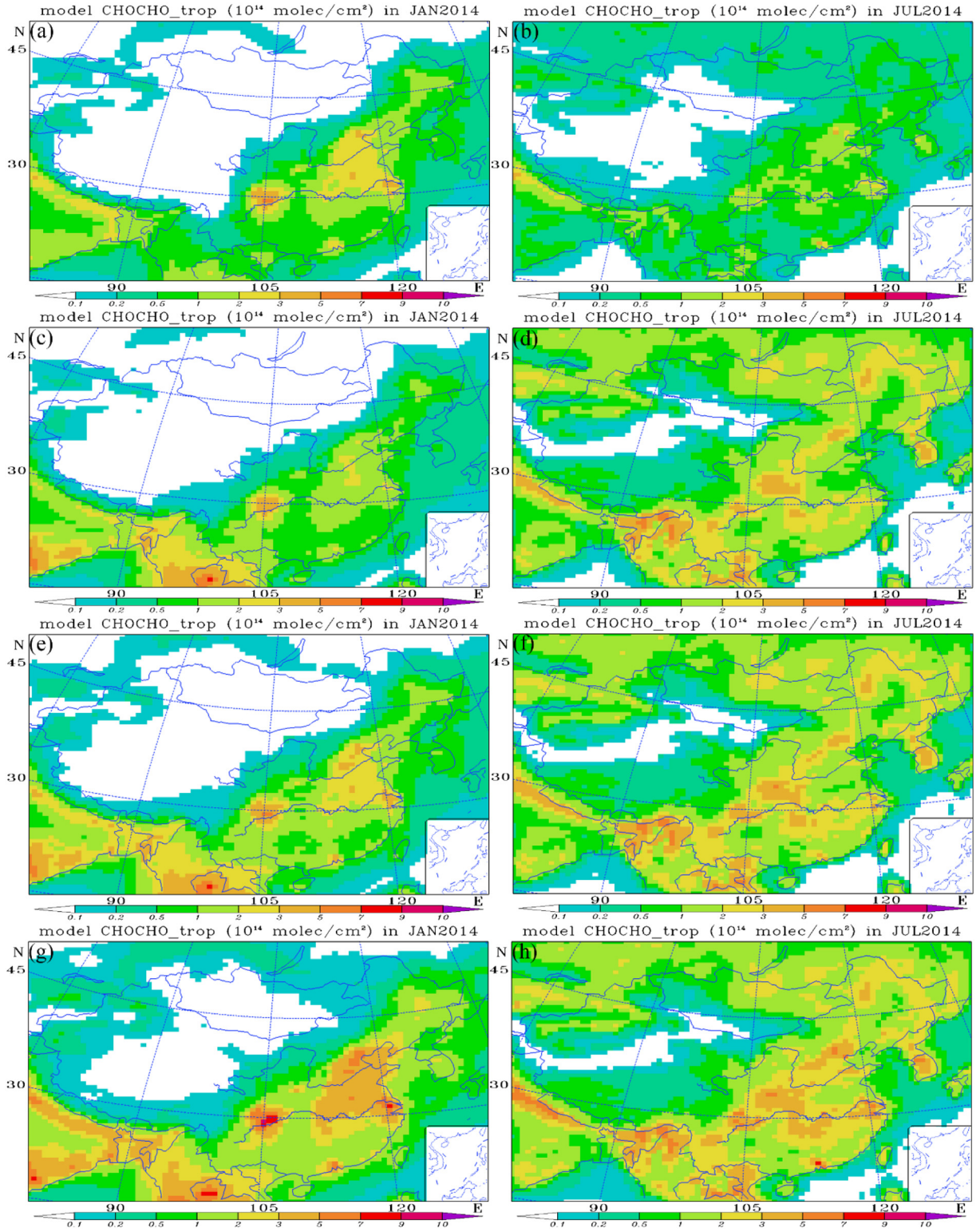

Fig. 5 – Distributions of monthly mean tropospheric glyoxal VCDs (molecules/cm^2) for the four sensitivity cases in January (left) and July (right) 2014: (a, b) case 1; (c, d) case 2; (e, f) case 3; (g, h) case 4. VCDs: vertical column densities.

January were almost within the reasonable range, and so were the emissions of ARO1 in July. However, further increases (a factor of 16) in the emissions of ARO2 in July (shown in Fig. S8a) did not improve the results as well as expected in the regions of the lower reaches of the Yangtze River and Yellow River, indicating the other missing source. But there were no significant biases between observed and base case simulated surface concentrations of ethylene and ALK2 (mainly originate from anthropogenic sources, shown in Fig. S9), indicating the reasonable emissions of these two precursors. Thus F2 was

Please cite this article as: Li, J., et al., Investigating missing sources of glyoxal over China using a regional air quality model (RAMS-CMAQ), J. Environ. Sci. (2018), https://doi.org/10.1016/j.jes.2018.04.021

taken into consideration and case 4 was devised with a two-fold increase in molar yields of glyoxal from aromatics, ethylene, and ALK2 based on case 3. The corresponding results are presented in Fig. 5g, h. Compared to the results for July, the improvements in the areas mentioned above were more obvious for January. The values over the high concentration regions were comparable to the observations, generally varying from 2×10^{14} to 5×10^{14} molecules/cm^2. However, the results in July of case 4 were similar to that shown in Fig. S8a and the concentrations of glyoxal column over the areas of the lower reaches of the Yangtze River and Yellow River were also not improved as much as expected. Based on the results, both the changes above in F1 and F2 were considered and the results were shown in Fig. S8b. As presented, the results were comparable to the observations especially in the areas of the lower reaches of the Yangtze River and Yellow River, indicating the possibilities that both F1 and F2 were underestimated. But there were still many uncertainties. For example, it was significant to increase the emissions of ARO2 by a factor of 16, which were then comparable to isoprene emission rate. But for the limitations of the observations, it was still hard to say that the emissions of ARO2 were not underestimated after such a significant increase, the uncertainties of which may also result in the underestimations in parts of regions between the lower reaches of the Yangtze River and Yellow River shown in Fig. S8b. In contrast, it was also possible that the emissions of ARO2 were overestimated after such a significant increase, which may cause the overestimations in some regions shown in Fig. S8b. Thus more observed concentrations of aromatic compounds as well as ethylene and ALK2 in different regions are needed to refine the results. Furthermore, there are no experimental evidences about the underestimations in the molar yields of glyoxal from anthropogenic precursors at the moment and the results were only obtained from the analyses in this study, which may also bring into large uncertainties. The further experimental studies and more detailed discussions are also needed to verify the results.

In conclusion, after the discussions in sensitivity cases above, there were much better agreements between the simulated glyoxal VCDs and the measurements. However, due to uncertainties in the individual glyoxal precursor emissions and the corresponding yields, the other potential sources and the uncertainties of the satellite retrievals of glyoxal, the model was still unable to fully reproduce the distributions and corresponding intensities of glyoxal column concentrations well. More work about the potential sources of glyoxal needs to be done in the future. Certainly, the impacts of the missing glyoxal concentrations on SOA simulations are also very valuable to be discussed in the further studies.

3. Conclusions

In this study, missing sources of glyoxal over China were investigated with the RAMS-CMAQ model in January and July 2014. To evaluate the influence on the modeled results from two potentially underestimated factors (namely, the emissions of aromatic compounds and the molar yields of glyoxal in the chemical mechanisms), four sensitivity simulations (cases 1 to 4) were performed and compared to satellite observations. The results showed that these two missing sources indeed had a significant impact. Due to the temporal and spatial variations of the dominant sources of precursors (anthropogenic or biogenic) across the region, the influences of the two factors showed apparent differences between January and July. The comparisons between the simulated and measured aromatic compound concentrations indicated an underestimation in the corresponding emissions. For case 1, improvements were seen in both months in areas with high anthropogenic emissions (*e.g.*, the NCP), and areas of high glyoxal VCDs became clearer and better reflect the measurements, implying that the emissions of aromatic compounds had previously been underestimated. The possibility of underestimated molar yields of glyoxal from isoprene was considered in case 2. The concentration results showed a stronger sensitivity to the mole yield changes in July than in January, due to the predominance of biogenic precursor emissions in the summer. Results in July were 3–5-fold higher than that in base case, which brought the simulated distributions of glyoxal column densities much closer to those of the measurements. As a result, the outputs from case 3 (in which both factors were considered) were similar to case 2, but with additional improvements over several high population density regions resulting from the increase in emissions of aromatic compounds, which were closer to the observations. However, not all the concentrations over high anthropogenic emissions regions were reproduced well, and case 4 expanded on case 3 by also considering the molar yields of glyoxal from anthropogenic precursors. With these additional mole yield changes, the concentrations agreed better with the measurements in regions of the lower reaches of the Yangtze River and Yellow River in January but not in July. More experimental studies and detailed discussions were needed in the future.

Although the modeled glyoxal VCDs were closer to the satellite observations after the discussions, biases still existed because of the uncertainties in the individual glyoxal precursor emissions, the corresponding yields, and other potential missing sources. Further work (such as additional ground and satellite measurements of glyoxal) will be needed to further improve our understanding of the emissions of the precursors, as well as the chemical mechanisms controlling the local glyoxal concentrations, as these factors have significant influences on the representation of glyoxal sources in the models.

Acknowledgments

This study was supported by the National Natural Science Foundation of China (No. 91544221), the National Key R&D Programs of China (Nos. 2017YFC0209803, 2017YFC0210000) and the CAS Strategic Priority Research Program Grant (No. XDB05020000). The contributions of the University of Bremen scientists to this manuscript are funded in part by the University and State of Bremen. Leonardo M. A. Alvarado gratefully acknowledges funding support by the German Academic Exchange Service (DAAD). Mihalis Vrekoussis acknowledges support from the DFG-Research Center/Cluster of Excellence “The Ocean in the Earth System-MARUM”.

Please cite this article as: Li, J., et al., Investigating missing sources of glyoxal over China using a regional air quality model (RAMS-CMAQ), J. Environ. Sci. (2018), https://doi.org/10.1016/j.jes.2018.04.021

Appendix A. Supplementary data

Supplementary data to this article can be found online at https://doi.org/10.1016/j.jes.2018.04.021.

REFERENCES

Altieri, K.E., Seitzinger, S.P., Carlton, A.G., Turpin, B.J., Klein, G.C., Marshall, A.G., 2008. Oligomers formed through in-cloud methylglyoxal reactions: chemical composition, properties, and mechanisms investigated by ultra-high resolution FT-ICR mass spectrometry. Atmos. Environ. 42, 1476–1490.

Alvarado, L.M.A., 2016. Investigating the role of glyoxal using satellite and MAX-DOAS measurements. (Ph.D. thesis). University of Bremen, Germany (http://elib.suub.uni-bremen.de/edocs/00105347-1.pdf).

Alvarado, L.M.A., Richter, A., Vrekoussis, M., Wittrock, F., Hilboll, A., Schreier, S.F., et al., 2014. An improved glyoxal retrieval from OMI measurements. Atmos. Meas. Tech. 7, 4133–4150.

Archibald, A.T., Cooke, M.C., Utembe, S.R., Shallcross, D.E., Derwent, R.G., Jenkin, M.E., 2010. Impacts of mechanistic changes on HOx formation and recycling in the oxidation of isoprene. Atmos. Chem. Phys. 10, 8097–8118.

Benkovitz, C.M., Scholtz, M.T., Pacyna, J., Tarrason, L., Dignon, J., Voldner, E.C., et al., 1996. Global gridded inventories of anthropogenic emissions of sulfur and nitrogen. J. Geophys. Res.-Atmos. 101, 29239–29253.

Boylan, J.W., Russell, A.G., 2006. PM and light extinction model performance metrics, goals, and criteria for three-dimensional air quality models. Atmos. Environ. 40, 4946–4959.

Butler, T.M., Taraborrelli, D., Fischer, C.B.H., Harder, H., Martinez, M., Williams, J., et al., 2008. Improved simulation of isoprene oxidation chemistry with the ECHAM5/MESSy chemistry-climate model: lessons from the GABRIEL airborne field campaign. Atmos. Chem. Phys. 8, 4529–4546.

Calvert, J.G., Atkinson, R., Kerr, J.A., Madronich, S., Moortgart, G.K., Wallington, T.J., et al. (Eds.), 2000. The Mechanisms of Atmospheric Oxidation of the Alkenes. Oxford University Press, pp. 401–412.

Calvert, J.G., Atkinson, R., Becker, K.H., Kamens, R.M., Seinfeld, J. H., Wallington, T.J., et al. (Eds.), 2002. The Mechanisms of Atmospheric Oxidation of Aromatic Hydrocarbons. Oxford University Press, Oxford.

Carlton, A.G., Turpin, B.J., Lim, H.J., Altieri, K.E., Seitzinger, S., 2006. Link between isoprene and secondary organic aerosol (SOA): pyruvic acid oxidation yields low volatility organic acids in clouds. Geophys. Res. Lett. 33, 272–288.

Carlton, A.G., Turpin, B.J., Altieri, K.E., Seitzinger, S., Reff, A., Lim, H.-J., et al., 2007. Atmospheric oxalic acid and SOA production from glyoxal: results of aqueous photooxidation experiments. Atmos. Environ. 41, 7588–7602.

Carlton, A.G., Turpin, B.J., Altieri, K.E., Seitzinger, S.P., Mathur, R., Roselle, S.J., et al., 2008. CMAQ model performance enhanced when in-cloud secondary organic aerosol is included: comparisons of organic carbon predictions with measurements. Environ. Sci. Technol. 42, 8798–8802.

Carlton, A.G., Wiedinmyer, C., Kroll, J.H., 2009. A review of secondary organic aerosol (SOA) formation from isoprene. Atmos. Chem. Phys. 9, 4987–5005.

Carter, W.P.L., 2000. Implementation of the SAPRC-99 Chemical Mechanism into the Models-3 Framework: Report to the US Environmental Protection Agency. Research Triangle Park, NC (Jan 29).

Chang, J.S., Brost, R.A., Isaksen, I.S.A., Madronich, S., Middleton, P., Stockwell, W.R., et al., 1987. A three-dimensional Eulerian acid deposition model: Physical concepts and formulation. J. Geophys. Res.-Atmos. 92, 14681–14700.

Cotton, W.R., Pielke, R.A., Walko, R.L., Liston, G.E., Tremback, C.J., Jiang, H., et al., 2003. RAMS 2001: current status and future directions. Meteorol. Atmos. Phys. 82, 5–29.

De Smedt, I., Stavrakou, T., Hendrick, F., Danckaert, T., Vlemmix, T., Pinardi, G., et al., 2015. Diurnal, seasonal and long-term variations of global formaldehyde columns inferred from combined OMI and GOME-2 observations. Atmos. Chem. Phys. 15, 12519–12545.

Emery, C., Tai, E., Yarwood, G., 2001. Enhanced meteorological modeling and performance evaluation for two Texas ozone episodes. Prepared for the Texas Natural Resource Conservation Commission, ENVIRON International Corporation, Novato, CA, USA.

Emmons, L.K., Walters, S., Hess, P.G., Lamarque, J.F., Pfister, G.G., Fillmore, D., et al., 2010. Description and evaluation of the model for ozone and related chemical tracers, version 4 (MOZART-4). Geosci. Model Dev. 3, 43–67.

Feng, T., Li, G., Cao, J., Bei, N., Shen, Z., Zhou, W., et al., 2016. Simulations of organic aerosol concentrations during springtime in the Guanzhong Basin, China. Atmos. Chem. Phys. 16, 10045–10061.

Fu, T.-M., Jacob, D.J., Wittrock, F., Burrows, J.P., Vrekoussis, M., Henze, D.K., 2008. Global budgets of atmospheric glyoxal and methylglyoxal, and implications for formation of secondary organic aerosols. J. Geophys. Res.-Atmos. 113.

Fu, T.M., Cao, J.J., Zhang, X.Y., Lee, S.C., Zhang, Q., Han, Y.M., et al., 2012. Carbonaceous aerosols in China: top-down constraints on primary sources and estimation of secondary contribution. Atmos. Chem. Phys. 12, 2725–2746.

Fuzzi, S., Andreae, M.O., Huebert, B.J., Kulmala, M., Bond, T.C., Boy, M., et al., 2006. Critical assessment of the current state of scientific knowledge, terminology, and research needs concerning the role of organic aerosols in the atmosphere, climate, and global change. Atmos. Chem. Phys. 6, 2017–2038.

Gao, M., Carmichael, G.R., Wang, Y., Saide, P.E., Yu, M., Xin, J., et al., 2016. Modeling study of the 2010 regional haze event in the North China Plain. Atmos. Chem. Phys. 16, 1673–1691.

Goldstein, A.H., Galbally, I.E., 2007. Known and unexplored organic constituents in the earth's atmosphere. Environ. Sci. Technol. 41, 1514–1521.

Gong, S.L., 2003. A parameterization of sea-salt aerosol source function for sub- and super-micron particles. Global Biogeochem. Cy. 17.

de Gouw, J.A., Middlebrook, A.M., Warneke, C., Goldan, P.D., Kuster, W.C., Roberts, J.M., et al., 2005. Budget of organic carbon in a polluted atmosphere: results from the New England Air Quality Study in 2002. J. Geophys. Res.-Atmos. 110.

Guenther, A.B., Jiang, X., Heald, C.L., Sakulyanontvittaya, T., Duhl, T., Emmons, L.K., et al., 2012. The model of emissions of gases and aerosols from nature version 2.1 (MEGAN2.1): an extended and updated framework for modeling biogenic emissions. Geosci. Model Dev. 5, 1471–1492.

Han, Z.W., Ueda, H., Matsuda, K., Zhang, R.J., Arao, K., Kanai, Y., et al., 2004. Model study on particle size segregation and deposition during Asian dust events in March 2002. J. Geophys. Res.-Atmos. 109.

Jiang, F., Liu, Q., Huang, X., Wang, T., Zhuang, B., Xie, M., 2012. Regional modeling of secondary organic aerosol over China using WRF/Chem. J. Aerosol Sci. 43, 57–73.

Juda-Rezler, K., Reizer, M., Huszar, P., Krueger, B.C., Zanis, P., Syrakov, D., et al., 2012. Modelling the effects of climate change on air quality over Central and Eastern Europe: concept, evaluation and projections. Clim. Res. 53, 179–203.

Kanakidou, M., Seinfeld, J.H., Pandis, S.N., Barnes, I., Dentener, F.J., Facchini, M.C., et al., 2005. Organic aerosol and global climate modelling: a review. Atmos. Chem. Phys. 5, 1053–1123.

Please cite this article as: Li, J., et al., Investigating missing sources of glyoxal over China using a regional air quality model (RAMS-CMAQ), J. Environ. Sci. (2018), https://doi.org/10.1016/j.jes.2018.04.021

Krotkov, N.A., McLinden, C.A., Li, C., Lamsal, L.N., Celarier, E.A., Marchenko, S.V., et al., 2016. Aura OMI observations of regional SO2 and NO2 pollution changes from 2005 to 2015. Atmos. Chem. Phys. 16, 4605–4629.

Kuhn, U., Andreae, M.O., Ammann, C., Araujo, A.C., Brancaleoni, E., Ciccioli, P., et al., 2007. Isoprene and monoterpene fluxes from Central Amazonian rainforest inferred from tower-based and airborne measurements, and implications on the atmospheric chemistry and the local carbon budget. Atmos. Chem. Phys. 7, 2855–2879.

Lelieveld, J., Butler, T.M., Crowley, J.N., Dillon, T.J., Fischer, H., Ganzeveld, L., et al., 2008. Atmospheric oxidation capacity sustained by a tropical forest. Nature 452, 737.

Lerot, C., Stavrakou, T., De Smedt, I., Muller, J.F., Van Roozendael, M., 2010. Glyoxal vertical columns from GOME-2 backscattered light measurements and comparisons with a global model. Atmos. Chem. Phys. 10, 12059–12072.

Levelt, P.F., Van den Oord, G.H.J., Dobber, M.R., Malkki, A., Visser, H., de Vries, J., et al., 2006. The ozone monitoring instrument. IEEE Trans. Geosci. Remote Sens. 44, 1093–1101.

Li, M., Zhang, Q., Streets, D.G., He, K.B., Cheng, Y.F., Emmons, L.K., et al., 2014. Mapping Asian anthropogenic emissions of non-methane volatile organic compounds to multiple chemical mechanisms. Atmos. Chem. Phys. 14, 5617–5638.

Li, J., Zhang, M., Wu, F., Sun, Y., Tang, G., 2017a. Assessment of the impacts of aromatic VOC emissions and yields of SOA on SOA concentrations with the air quality model RAMS-CMAQ. Atmos. Environ. 158, 105–115.

Li, M., Zhang, Q., Kurokawa, J.-i., Woo, J.-H., He, K., Lu, Z., et al., 2017b. MIX: a mosaic Asian anthropogenic emission inventory under the international collaboration framework of the MICS-Asia and HTAP. Atmos. Chem. Phys. 17, 935–963.

Lim, Y.B., Ziemann, P.J., 2005. Products and mechanism of secondary organic aerosol formation from reactions of n-alkanes with OH radicals in the presence of NOx. Environ. Sci. Technol. 39, 9229–9236.

Lin, J., An, J., Qu, Y., Chen, Y., Li, Y., Tang, Y., et al., 2016. Local and distant source contributions to secondary organic aerosol in the Beijing urban area in summer. Atmos. Environ. 124 (Part B), 176–185.

Liu, Z., Wang, Y., Vrekoussis, M., Richter, A., Wittrock, F., Burrows, J.P., et al., 2012. Exploring the missing source of glyoxal (CHOCHO) over China. Geophys. Res. Lett. 39.

Matsui, H., Koike, M., Kondo, Y., Takami, A., Fast, J.D., Kanaya, Y., et al., 2014. Volatility basis-set approach simulation of organic aerosol formation in East Asia: implications for anthropogenic–biogenic interaction and controllable amounts. Atmos. Chem. Phys. 14, 9513–9535.

Myriokefalitakis, S., Vrekoussis, M., Tsigaridis, K., Wittrock, F., Richter, A., Bruehl, C., et al., 2008. The influence of natural and anthropogenic secondary sources on the glyoxal global distribution. Atmos. Chem. Phys. 8, 4965–4981.

Peeters, J., Muller, J.-F., 2010. HOx radical regeneration in isoprene oxidation via peroxy radical isomerisations. II: experimental evidence and global impact. Phys. Chem. Chem. Phys. 12, 14227–14235.

Peeters, J., Nguyen, T.L., Vereecken, L., 2009. HOx radical regeneration in the oxidation of isoprene. Phys. Chem. Chem. Phys. 11, 5935–5939.

Randerson, J.T., van der Werf, G.R., Giglio, L., Collatz, G.J., Kasibhatla, P.S., 2015. Global fire emissions database, version 4 (GFEDv4). ORNL DAAC, Oak Ridge, Tennessee, USA https://doi.org/10.3334/ORNLDAAC/1293.

Seinfeld, J.H., Pankow, J.F., 2003. Organic atmospheric particulate material. Annu. Rev. Phys. Chem. 54, 121–140.

Stavrakou, T., Mueller, J.F., De Smedt, I., Van Roozendael, M., Kanakidou, M., Vrekoussis, M., et al., 2009. The continental source of glyoxal estimated by the synergistic use of spaceborne measurements and inverse modelling. Atmos. Chem. Phys. 9, 8431–8446.

Stavrakou, T., Peeters, J., Muller, J.F., 2010. Improved global modelling of HOx recycling in isoprene oxidation: evaluation against the GABRIEL and INTEX-A aircraft campaign measurements. Atmos. Chem. Phys. 10, 9863–9878.

Sun, J., Wu, F., Hu, B., Tang, G., Zhang, J., Wang, Y., 2016. VOC characteristics, emissions and contributions to SOA formation during hazy episodes. Atmos. Environ. 141, 560–570.

Utembe, S.R., Cooke, M.C., Archibald, A.T., Shallcross, D.E., Derwent, R.G., Jenkin, M.E., 2011. Simulating secondary organic aerosol in a 3-D Lagrangian chemistry transport model using the reduced common representative Intermediates mechanism (CRI v2-R5). Atmos. Environ. 45, 1604–1614.

Volkamer, R., Jimenez, J.L., San Martini, F., Dzepina, K., Zhang, Q., Salcedo, D., et al., 2006. Secondary organic aerosol formation from anthropogenic air pollution: rapid and higher than expected. Geophys. Res. Lett. 33.

Vrekoussis, M., Wittrock, F., Richter, A., Burrows, J.P., 2009. Temporal and spatial variability of glyoxal as observed from space. Atmos. Chem. Phys. 9, 4485–4504.

Vrekoussis, M., Wittrock, F., Richter, A., Burrows, J.P., 2010. GOME-2 observations of oxygenated VOCs: what can we learn from the ratio glyoxal to formaldehyde on a global scale? Atmos. Chem. Phys. 10, 10145–10160.

Wittrock, F., Richter, A., Oetjen, H., Burrows, J.P., Kanakidou, M., Myriokefalitakis, S., et al., 2006. Simultaneous global observations of glyoxal and formaldehyde from space. Geophys. Res. Lett. 33.

Wu, F., Yu, Y., Sun, J., Zhang, J., Wang, J., Tang, G., et al., 2016. Characteristics, source apportionment and reactivity of ambient volatile organic compounds at Dinghu Mountain in Guangdong Province, China. Sci. Total Environ. 548, 347–359.

Zhang, H., Kamens, R.M., 2012. The influence of isoprene peroxy radical isomerization mechanisms on ozone simulation with the presence of NOx. J. Atmos. Chem. 69, 67–81.

Zhang, H., Ying, Q., 2011. Secondary organic aerosol formation and source apportionment in Southeast Texas. Atmos. Environ. 45, 3217–3227.

Zhao, J., Levitt, N.P., Zhang, R., Chen, J., 2006. Heterogeneous reactions of methylglyoxal in acidic media: implications for secondary organic aerosol formation. Environ. Sci. Technol. 40, 7682–7687.

Please cite this article as: Li, J., et al., Investigating missing sources of glyoxal over China using a regional air quality model (RAMS-CMAQ), J. Environ. Sci. (2018), https://doi.org/10.1016/j.jes.2018.04.021